Research Article

Latif Ahmad, Shah Islam, Muhammad Yasir, Umair Khan*, and Jomana A. Bashatah

Spinning dynamics of stress-dependent viscosity of generalized Cross-nonlinear materials affected by gravitationally swirling disk

https://doi.org/10.1515/phys-2025-0169
received February 21, 2025; accepted May 19, 2025

Abstract: Practical fields, including materials processing, space technology, ocean technology, and many mechanical machineries, play a major part in advancing the modern world. Lack of energy production and energy reduction have been noticed as one of the main challenges in recent decades. To properly address this, one should need to modify the thermal characteristics of traditional materials with different surface dynamics involvement. The present investigation examines the heat transfer performance and pumping power of destructive flow patterns of rheological materials caused by viscous stress is significant due to physical aspects. One key objective is to demonstrate the conversion of kinetic energy into internal energy, highlighting its applications across various fields of engineering, science, and technology. The current study is about to address the impacts of viscous stress, stagnation point, gravity, slip flow, and thermal slip in the typical swirling motion of Cross liquid. The main problem that arises from these physical aspects is presented in the form of dimensionless mathematical equations. The flow problem configured in this study is based on the higher viscous forces and lower inertial forces. The leading dimensionless equations are formulated by using the Lie symmetry analysis. A well-known modified collocation formula is used to examine the higher radial flow speed of the material with the parallel variation in the Richardson number, and the other components decline with the same variation. The temperature of the dissipated materials is enhanced by considering the higher values of the Eckert number. Time relaxation caused a reduction in the resistance forces in the r-direction and is noticed with the opposite trend in the case of θ-direction which is more prominent. An excellent agreement is observed by introducing a comparison with the existing works.

Keywords: Thermally radiated flow, rotational motion, Cross liquid, stagnation point, viscus dissipation, mixed convection

1 Introduction

A non-Newtonian fluid is a type of fluid whose viscosity changes based on the applied stress or force. Non-Newtonian fluids have a wide range of applications, including food processing, industrial processes (such as drilling fluids), starch suspension, toothpaste, shampoo, ketchup, custard, *etc.* The behavior of non-Newtonian fluids has been extensively studied by numerous researchers. For instance, over the surface of an elastic medium, the steady-based dynamical behavior of a non-Newtonian fluid was discussed by Bilal *et al.* [1]. With the consideration of permeable channel walls, the purpose of Qureshi *et al.*'s [2] work was to deliberate the flow characteristics of a Casson nanofluid. The characteristic of Brownian and thermophores motion for nanosized particles of Casson fluid flow problem over a semi-infinite disk was introduced by Rehman *et al.* [3]. However, the flow analysis caused by a solid rotating disk is extensively recognized by various researchers, and scientists like Kármán [4] initially examined the viscous fluid flow caused by a rotating solid disk. Von Karman initially introduced and considered a special transformation (Von Karman transformation). These transformations are executed to convert the basic Navier Stokes equations in terms of partial differential equations into ordinary differential equations. After this work, many researchers carried out the characteristic and modeling of both Newtonian and non-Newtonian

* **Corresponding author: Umair Khan,** Department of Mathematics, Saveetha School of Engineering, Saveetha Institute of Medical and Technical Sciences, Saveetha University, Chennai, 602105, Tamil Nadu, India; Department of Mathematics, Faculty of Science, Sakarya University, Serdivan/Sakarya, 54050, Turkey,
e-mail: umairkhan@sakarya.edu.tr
Latif Ahmad, Shah Islam: Department of Mathematics, Shaheed Benazir Bhutto University, Sheringal Dir Upper, 18000, Pakistan
Muhammad Yasir: Department of Mathematics, Quaid-i-Azam University, Islamabad, 44000, Pakistan
Jomana A. Bashatah: Department of Industrial and Systems Engineering, College of Engineering, Princess Nourah bint Abdulrahman University, P.O. Box 84428, Riyadh 11671, Saudi Arabia

fluid over a swirling disk. The Von Karman work is further extended by Turkyilmazoglu and Senel [5]. Ahmed *et al.* [6] studied fluid flow with nanoparticle over a spinning surface affected by temperature and chemical reaction. In a stretching porous medium ternary composition with considering the impact of heat generation bioconvective nanofluid flow was investigated by Arafa *et al.* [7]. Turkyilmazoglu [8] analyzed heat and mass transfer in electrically conducting fluid flow over a porous rotating disk, considering Hall current effects.

The Cross fluid [9] is a generalized fluid that refers to a type of fluid that exhibits a non-Newtonian behavior while still adhering to certain aspects of Newtonian fluid behavior under certain conditions. Generalized Newtonian fluids (GNF) can be found in various industries, including lubricants, artificial organs, the oil and gas industry, aerodynamics, *etc.* Understanding their behavior is crucial for designing processes and equipment that handle these fluids efficiently. A revolving disk with the presence of power-law fluid flow was inspected by Andersson *et al.* [10]. Khan *et al.* [11] examined the physical features of Carreau liquid over an irregularly textured surface when different molecule orientations were present. A generalized characteristic of fluid thermal conductivity and heat transfer assessment of a Carreau liquid regarding a rotating disk was disclosed by Ming *et al.* [12]. The combination of free and forced convection heat transfer process is known as mixed convection, which is used in a lot of industrial and engineering applications like heat exchangers, radiators of automobiles, nuclear reactors, cooling of electronic devices, food and chemical processing, and solar collectors. Several scholars are studying the structure of complicated flow systems, such as vented enclosures, to use them to cool electronic equipment [13–15]. In wavy wall, Abu-Nada and Chamkha [16] investigated the mixed convection laminar time-independent flows taking water-CuO nano-fluid in a lid-driven cavity. Kalteh *et al.* [17] explored the convection heat transfer along with the effects of nanomaterial thickness and volume fraction. For enhancement of the Richardson number, they used different nanomaterials such as TiO_2, Al_2O_3, CuO, and Ag in base fluid (water). In a square cavity that is heated, Garoosi *et al.* [18] examined the heat transfer rates of Al_2O_3-water nanofluid under mixed and natural convection conditions. Turkyilmazoglu and Pop [19] analyzed the behavior of Bingham fluid which flow when a certain force is applied considering stretching and rotating geometry. Yasmin *et al.* [20] studied the flow of a special blood-based fluid with nanoparticles over a heated surface in a porous material.

The velocity slip is defined as the velocity difference between the fluid and the surface is called the slip velocity. For instance, if a disk rotates and the fluid near the surface does not move at the disk's speed, the difference is the slip velocity. Velocity slip is relevant in various contexts, such as fluid flow over surfaces, lubrication, and aerodynamics. Thermal slip refers to the phenomenon where there is a difference in temperature between a fluid and a solid surface it is in contact with, and the heat transfer between them does not occur perfectly. This may lead to a temperature gradient or variations in heat flux across the interface. Thermal slip is important in various applications, including heat exchangers, electronic cooling, and boundary layer studies in aerodynamics. Many researchers explain the velocity and thermal slip in fluid flow. For instance, in fluid flow, the linear velocity slip boundary condition (BC) was studied by Navier [21]. Maxwell [22] showed that temperature variations in rarefied gas were the origin of the velocity slip BC in the study of stress. Hayat *et al.* [23] focused on how velocity slips under a magnetic field and with conductivity depending on temperature, initiated by the expansion of a cylindrical object, and noted that the resultant number boosts with the increase in the velocity slip parameter. Mathur *et al.* [24] analyzed the development of velocity slip in a micropolar nanofluid. Additionally, Motsa *et al.* [25] studied the stagnation point flow of Maxwell material over a shrinking surface. Turkyilmazoglu [26] investigated the dynamics of slip flow and heat exchange between two corotating disk. Yasmin *et al.* [27] investigated water-based nanofluid flow with carbon nanotubes over a stretching surface, with considering slip and heat transfer. Asghar *et al.* [28] investigated the electrically conducted ferrofluid flow including slip condition over a shrinking/stretching surface.

Viscous dissipation is the process in which the kinetic energy of a fluid flow is transformed into thermal energy as a result of viscous forces. This phenomenon is particularly significant in flows with high velocities or in fluids with high viscosity. Viscous dissipation plays an important role in various fields including heat transfer in slurries, geothermal energy, aerodynamics and aircraft design, turbine and engine efficiency, *etc.* The importance of viscous dissipative in the form of heat flow and isothermal in the plate in free convection was studied by Gupta [29]. Effects of viscous consumption on a winding surface in external natural convection were reported by Gebhart and Mollendorf [30]. Boutoutaou and Fontaine [31] reported the flow of power law fluid filled in a micro-cylinder. Sondalgekar and Murty [32] analyzed two dimensional unstable heat flow on an infinite porous vertical plate. In a convective spinning rigid disk, the impact of ohmic heating on radiative viscoelastic nanofluid flow was considered by Ahmed *et al.* [33]. Ontela *et al.* [34] analyzed and optimized the movement of microorganism in a nanofluid flow with elastic properties over a spinning disk. Ali *et al.* [35]

analyzed the numerical investigation for viscoelastic fluid with heat transfer analysis during rollover-web coating phenomena. This study can further extend in the directions as presented by many researchers [36–38].

Keeping in view these aspects regarding the dynamics and physical analysis of such complex nature materials, we can extend this work in the directions and works presented in previous studies [39,40]. Because these works are mostly relevant in order to explore the different unique features of the generalized materials while applying the said approaches.

1.1 Novelty

As per the aforementioned literature, the rheological study of Cross materials with magnetohydrodynamics (MHD) stagnation point, viscous dissipation, and mixed convection in the spinning or rotational devices has not been brought under consideration. Moreover, a remarkable influence of the gravity factor due to a vertically rotating disk is another new attempt. The flow velocity and temperature are considered for the first time with the significant influence of thermally and dynamically slipped rotating disk filled with Cross liquid. From application perspective, this work has a wide range of applications in those areas of modern arena where the optimized heat transfer is declared as an essential need.

1.2 Significance and objectives

- To examine the rheological nature of Cross fluid flow with gravitationally affected swirling disk.
- To explore the unique nature of the stagnation points, flow of Cross liquid placed on moving disk.
- To present the thermal and velocity slips of the materials on a spinning disk.
- To portray the destructive flow situation with the variable involvement of viscous forces.

1.3 Physical interpretation and assumptions

A disk is fixed vertically as shown in Figure 1 and rotating with angular velocity Ω, which is assumed realistically. The shear stress-dependent viscosity of Cross liquid is assumed to portray the unique rheology of the materials. The heat and mass flows are formulated with the assumption of

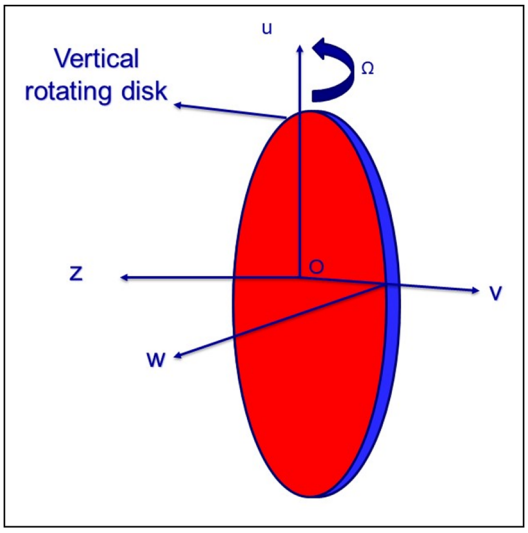

Figure 1: Physical interpretation.

mixed convection and viscous dissipation. The disk is assumed to have an anticlockwise swirling motion having velocity field $\mathbf{V} = [u(r, z), v(r, z), w(r, z)]$. The surface temperature T_w and concentration C_w are effectively differentiated from the infinite temperature T_∞ and concentration C_∞. This unique work produced the vector form of mathematical equations, *i.e.*, momentum, energy, and concentration while using cylindrical coordinates.

$$\nabla\cdot \boldsymbol{V} = 0, \tag{1}$$

$$\rho(\boldsymbol{V}\cdot\nabla\boldsymbol{V}) = -\nabla P + \nabla\cdot\tau + gB_T\rho(T - T_\infty) + gB_C\rho(C - C_\infty) - \sigma B_O^2(U - u), \tag{2}$$

$$\rho c_P(\boldsymbol{V}\cdot\nabla T) = \nabla\cdot(k\nabla T), \tag{3}$$

$$(\boldsymbol{V}\cdot\nabla C) = \nabla\cdot(D\nabla C). \tag{4}$$

where the velocity vector is $\mathbf{V}$, ρ is the density, P is the pressure, c_p is the specific heat, and τ [9] is the stress tensor.

$$\frac{\partial}{\partial r}u + \frac{\partial}{\partial z}w + \frac{1}{r}v = 0, \tag{5}$$

$$\left\{\begin{array}{l}\rho\left[u\dfrac{\partial u}{\partial r} + w\dfrac{\partial u}{\partial z} - \dfrac{v^2}{r}\right] = -\dfrac{\partial}{\partial r}p + \dfrac{\partial}{\partial z}(\tau_{rz}) + \dfrac{1}{r}\dfrac{\partial}{\partial r}(r\tau_{rr}) \\ \dfrac{\tau_{\theta\theta}}{r} + gB_T\rho(T - T_\infty) + gB_c\rho(C - C_\infty) - \sigma B_o^2(U - u)\end{array}\right\}, \tag{6}$$

$$\rho\left[u\frac{\partial}{\partial r}v + w\frac{\partial}{\partial z}v + \frac{u}{r}v\right] = \frac{\partial}{\partial z}(\tau_{z\theta}) + \frac{\tau_{\theta r} - \tau_{r\theta}}{r} + \frac{1}{r^2}\frac{\partial}{\partial r}(r^2\tau_{r\theta}) - \sigma B_o^2 v, \tag{7}$$

$$\rho\left[w\frac{\partial}{\partial z}w + u\frac{\partial}{\partial r}w\right] = -\frac{\partial}{\partial z}p + \frac{\partial}{\partial z}(\tau_{zz}) + \frac{1}{r}\frac{\partial}{\partial r}(r\tau_{rz}), \tag{8}$$

$$\left\{\rho C_p\left[w\frac{\partial}{\partial z}T + u\frac{\partial}{\partial r}T\right] = \frac{\partial}{\partial r}\left(k\frac{\partial}{\partial r}T\right) + \frac{\partial}{\partial z}\left(k\frac{\partial}{\partial z}T\right) + \frac{k}{r}\frac{\partial}{\partial r}T + \mu\left(\left(\frac{\partial v}{\partial r}\right)^2 + \left(\frac{\partial u}{\partial r}\right)^2\right)\right\}, \tag{9}$$

$$w\frac{\partial}{\partial z}C + u\frac{\partial}{\partial r}C = D_B\left[\frac{\partial}{\partial r}\left(\frac{\partial}{\partial r}C\right) + \frac{1}{r}\frac{\partial}{\partial r}C + \frac{\partial}{\partial z}\left(\frac{\partial}{\partial z}C\right)\right], \tag{10}$$

where σ, B_o, D_B are the electrical conductivity, magnetic field, and diffusion coefficient, respectively.

The non-zero components of the tensor are deliberated as follows:

$$\tau_{rr} = \frac{\partial u}{\partial r},\ \tau_{rz} = \frac{\frac{\partial}{\partial z}(u) + \frac{\partial}{\partial z}(w)}{2},\ \tau_{\theta\theta} = \frac{u}{r},\ \tau_{\theta r} = \left(\frac{r}{2}\right)\frac{\partial}{\partial r}\left(\frac{v}{r}\right),\ \tau_{z\theta} = \left(\frac{1}{2}\right)\left(\frac{\partial v}{\partial z}\right), \tag{11}$$

where the dynamic viscosity (μ) for the rheology of Cross fluid [9] is given by

$$\left\{\mu = \mu_\infty + (\mu_o - \mu_\infty)\left[\frac{1}{1 + (\Gamma\dot{\gamma})^n}\right]\right\}. \tag{12}$$

The newly proposed BCs are as follows:

$$\left\{\begin{array}{l} z = 0\ :\ w = 0,\ v = r\Omega,\ u = L_1\dfrac{\partial u}{\partial z},\ C = C_w, \\ T = L_2\dfrac{\partial T}{\partial z} \\ z \to z_\infty\ :\ v \to 0,\ u \to U = r\Omega,\ C \to C_\infty,\ T \to T_\infty \end{array}\right\}. \tag{13}$$

Where L_1 and L_2 are the velocity and thermal slip, respectively.

Letting [12]:

$$\bar{r} = \frac{r}{R},\ \bar{z} = \frac{z\,\mathrm{Re}^{\frac{1}{2}}}{R},\ \bar{u} = \frac{u}{\Omega R},\ \bar{v} = \frac{v}{\Omega R},\ \bar{w} = \frac{w\,\mathrm{Re}^{\frac{1}{2}}}{\Omega R},$$
$$\bar{p} = \frac{p\,\mathrm{Re}}{\rho\Omega^2R^2},\ \bar{\Gamma} = \Omega\Gamma\,\mathrm{Re}^{\frac{1}{2}},$$
$$\bar{\mu} = \frac{\mu}{\mu_o},\ \bar{\lambda} = \Omega\lambda\,\mathrm{Re}^{\frac{1}{2}},\ \bar{T} = \frac{T - T_\infty}{T_w - T_\infty},\ \bar{C} = \frac{C - C_\infty}{C_w - C_\infty}. \tag{14}$$

Using Eq. (13), Eqs. (5)–(13) can be transformed into the following forms:

$$\left\{\frac{\partial}{\partial\bar{z}}\bar{w} + \frac{1}{\bar{r}}\bar{v} + \bar{u}\frac{\partial}{\partial\bar{r}}\bar{u} = 0\right\}, \tag{15}$$

$$\bar{w}\frac{\partial}{\partial\bar{z}}\bar{u} - \frac{1}{\bar{r}}\bar{v}^2 + \bar{u}\frac{\partial}{\partial\bar{r}}\bar{u} = \frac{\partial}{\partial\bar{z}}\left(\bar{\mu}\frac{\partial}{\partial\bar{z}}\bar{u}\right) - M(\bar{U} - \bar{r}) + Ri(\bar{T} - Nc\bar{C}), \tag{16}$$

$$\bar{u}\frac{\partial}{\partial\bar{r}}\bar{v} + \bar{w}\frac{\partial}{\partial\bar{z}}\bar{v} + \frac{\bar{u}}{\bar{r}}\bar{v} = \frac{\partial}{\partial\bar{z}}\left(\bar{\mu}\frac{\partial}{\partial\bar{z}}\bar{v}\right) - M\bar{v}, \tag{17}$$

$$\bar{w}\frac{\partial}{\partial\bar{z}}\bar{w} + \bar{u}\frac{\partial}{\partial\bar{r}}\bar{w} = -\frac{\partial}{\partial\bar{z}}\bar{p} + 2\frac{\partial}{\partial\bar{z}}\left(\bar{\mu}\frac{\partial}{\partial\bar{z}}\bar{w}\right) + \frac{1}{\bar{r}}\frac{\partial}{\partial\bar{r}}\left(\bar{r}\bar{\mu}\left(\frac{\partial}{\partial\bar{z}}\bar{u}\right)\right), \tag{18}$$

$$\bar{w}\frac{\partial}{\partial\bar{z}}\bar{T} + \bar{u}\frac{\partial}{\partial\bar{r}}\bar{T} = \frac{1}{\mathrm{Pr}} + \frac{\partial^2}{\partial\bar{z}^2}\bar{T} + \mathrm{Ec}\bar{\mu}\left(\left(\frac{\partial\bar{v}}{\partial\bar{z}}\right)^2 + \left(\frac{\partial\bar{u}}{\partial\bar{z}}\right)^2\right), \tag{19}$$

$$\bar{w}\frac{\partial}{\partial\bar{z}}\bar{C} + \bar{u}\frac{\partial}{\partial\bar{r}}\bar{C} = \frac{1}{\mathrm{Sc}}\frac{\partial^2}{\partial\bar{z}^2}\bar{C}, \tag{20}$$

the dimensionless form of tensor (μ) is stated as

$$\bar{\mu} = \left[1 + \Gamma_r^2\left[\left(\frac{\partial\bar{v}}{\partial\bar{z}}\right)^2 + \left(\frac{\partial\bar{u}}{\partial\bar{z}}\right)^2\right]^{\frac{n}{2}}\right]^{-1}. \tag{21}$$

where (Ri) is the Richardson number, Schmidt number is deliberated by $\mathrm{Sc} = \left(\frac{v}{D_B}\right)$, $M = \frac{\sigma B_o^2}{\Omega\rho}$ is the magnetic parameter, $\mathrm{Ec} = \frac{\Omega^2R^2}{C_pr^2(T_w - T_\infty)}$ is the Eckert number, (Nc) is the Buoyancy-ratio parameter, and $\mathrm{Pr} = \left(\frac{\rho C_p\nu}{k}\right)$ is Prandtl number.

To non-dimensionalize the governing equations, the following variables [12] are used:

$$\{\eta = \bar{z},\ \bar{p} = Q(\eta),\ \bar{w} = H(\eta),\ \bar{u} = \bar{r}F(\eta),\ \bar{v} = \bar{r}G(\eta),\ \bar{T} = \theta(\eta),\ \bar{C} = \varphi(\eta)\}. \tag{22}$$

By using Eq. (22), Eqs. (15)–(21) take the following form:

$$2F + H' = 0, \tag{23}$$

$$(A + ABF'^2)F'' - F^2 + G^2 - HF' + ABF'G'G'' + R_i(\theta + \mathrm{Nc}\varphi) - M(F - 1) = 0, \tag{24}$$

$$ABF'F''G' + ABG'^2G'' + AG'' - 2FG - HG' - MG = 0, \tag{25}$$

$$\left\{\begin{array}{c} ABF'(F'^2 + G'^2) + 2AF' \\ + 2ABH'(F'F'' + G'G'') + 2AH'' - HH' - Q' = 0 \end{array}\right\}, \tag{26}$$

$$H\theta' - \frac{1}{p_r}[AB(F'F'' + G'G'')\theta' + A\theta''] + \mathrm{Ec}A(F'^2 + G'^2) = 0, \tag{27}$$

$$H\varphi' = \frac{1}{\mathrm{Sc}}\varphi'', \tag{28}$$

where

$$\mu = \left[1 + [\Gamma_r^2(F'^2 + G'^2)]^{\frac{n}{2}}\right]^{-1}. \tag{29}$$

where

$$A = \left[1 + (\Gamma_r^2(F'^2 + G'^2))^{\frac{n}{2}}\right]^{-1}, \tag{30}$$

Table 1: Comparative values for $\Gamma = 0$ and $\Pr = n = 1$

Physical quantities	Anderson *et al.* [10]	Khan *et al.* [11]	Ming *et al.* [12]	Current results
$F'(0)$	0.510	0.5102	0.5102320	0.510235189
$-G'(0)$	0.616	0.6159	0.6159216	0.615921929
$-H(\infty)$	0.883	—	0.8843802	0.884378965
$-\theta'(0)$	0.396	—	0.3962493	0.391064518

and

$$B = -n\overline{\Gamma}_r^2(\Gamma_r^2(F'^2 + G'^2))^{\frac{n-2}{2}} \cdot \left[1 + (\Gamma_r^2(F'^2 + G'^2))^{\frac{n}{2}}\right]^{-1}. \quad (31)$$

Conditions with transformed form are deliberated as follows:

$$\left\{\begin{array}{l} \eta = 0: \quad F = \lambda_1 F', \ G = 1, \ H = 0, \ \theta = \lambda_2 \theta', \ \varphi = 1 \\ \eta \to \infty: \quad F = 1, \ G = H = \theta = Q = \varphi = 0 \end{array}\right\}. \quad (32)$$

In the above equation, $\lambda_1 = \frac{L_{1\varrho}}{\upsilon}$ and $\lambda_2 = \frac{L_{2\varrho}}{\upsilon}$ are the velocity and thermal slips, respectively.

1.4 Practical quantities

The associated physical quantities for Cross liquid are expressed as:

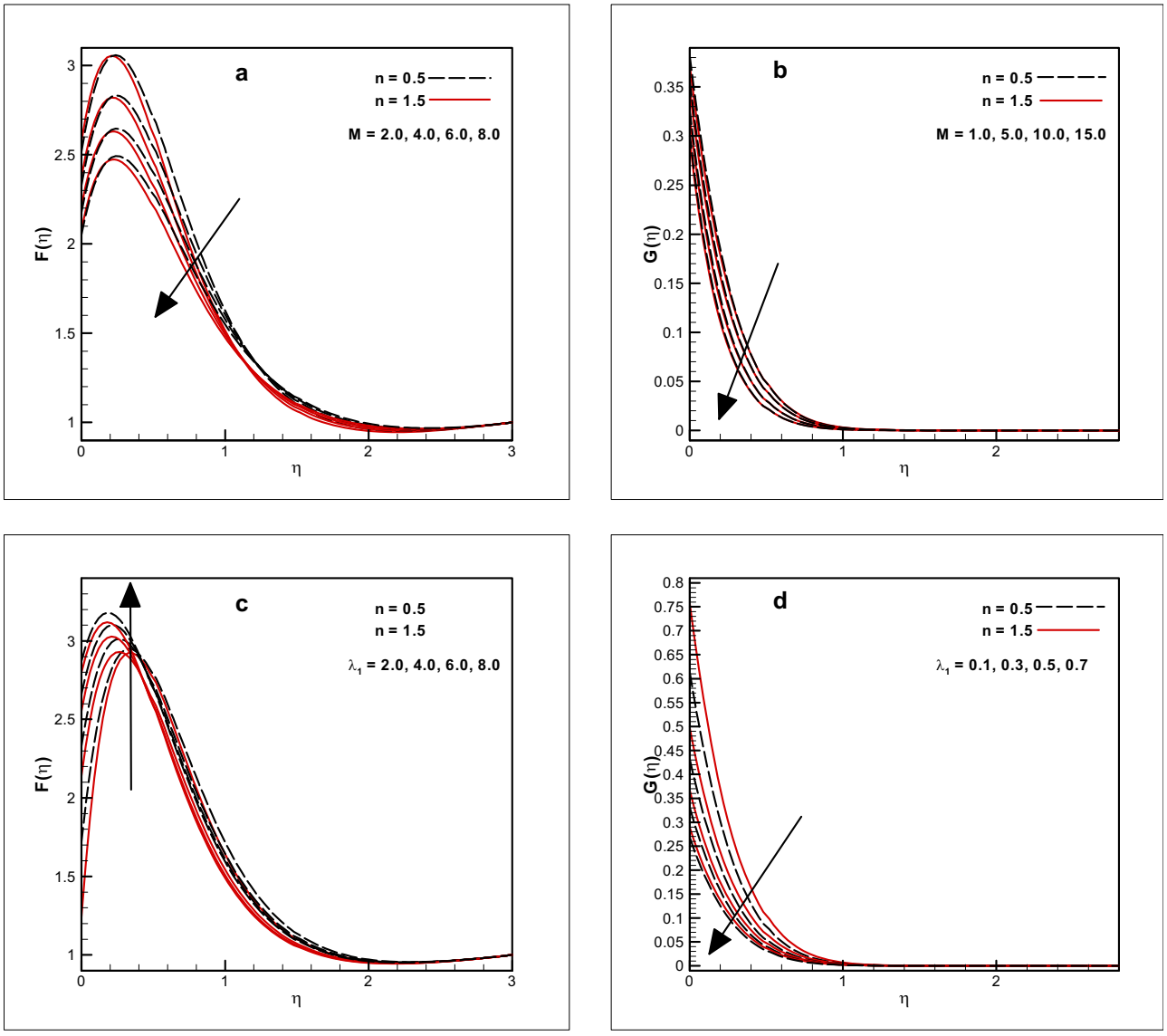

Figure 2: (a)–(d) Impact of M and λ_1 on (η) and $G(\eta)$.

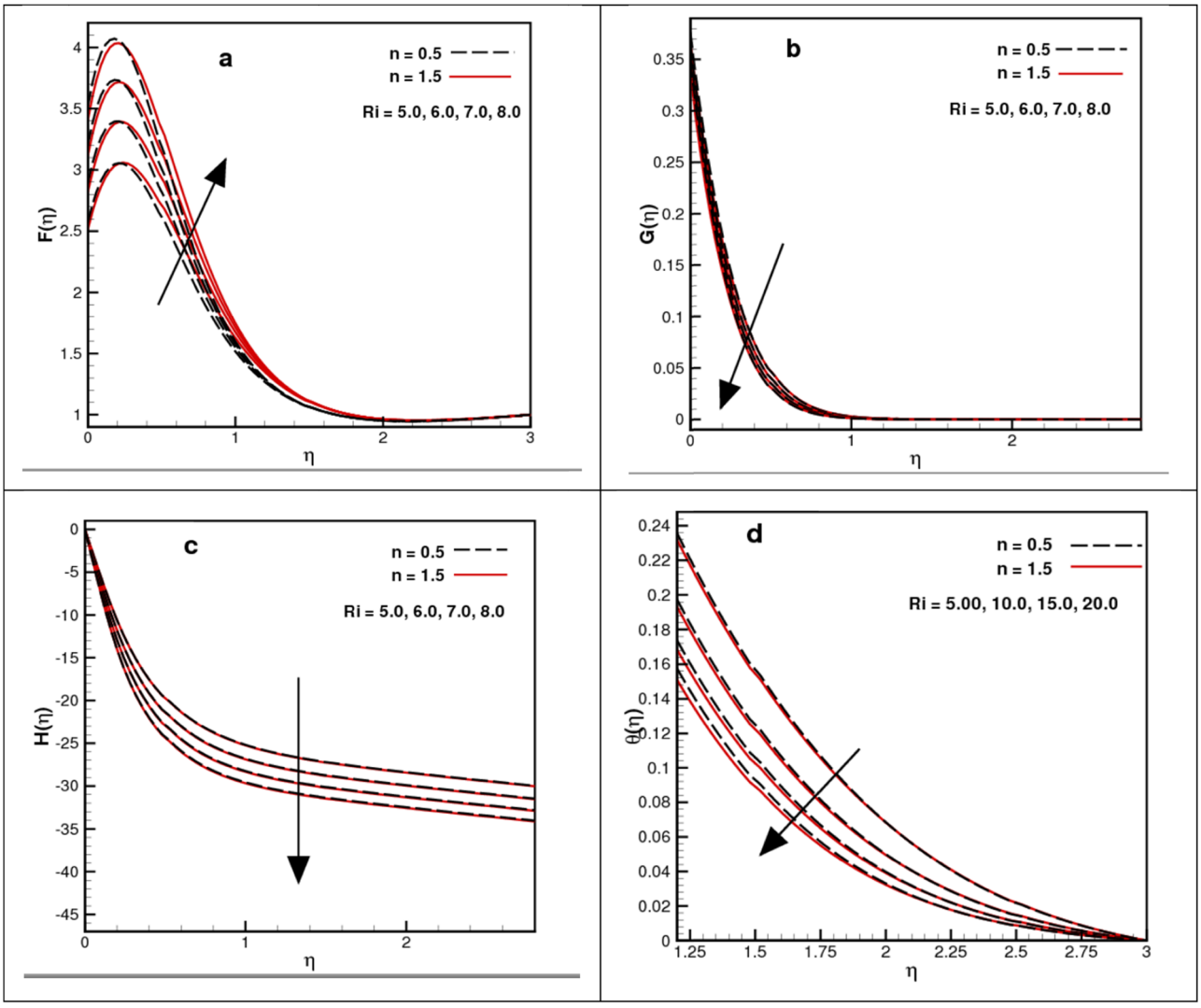

Figure 3: Impact of Ri on (a) $F(\eta)$, (b) $G(\eta)$, (c) $H(\eta)$, and (d) $\theta(\eta)$.

1.4.1 Drage coefficients

$$\left\{\begin{array}{l} C_{fr} = \dfrac{\tau_{rz}}{l(r\theta)^2} \text{ drag coefficient in } r\text{-direction} \\ C_{f\ \theta} = \dfrac{\tau_{z\theta}}{l(r\Omega)^2} \text{ drag coefficient in } \theta\text{-direction} \end{array}\right\}. \quad (33)$$

1.4.2 Heat flow rate

$$\mathrm{Nu} = \frac{rq_n}{k(T_w - T_\infty)} \text{heat flow rate in } r\text{-direction}. \quad (34)$$

1.4.3 Mass flow rate

$$\mathrm{Sh} = \frac{rj_n}{k(C_w - C_\infty)}, \quad (35)$$

where l is the characteristic length, the heat and mass fluxes are defined as $q_n = -k\partial T/\partial z$ and $j_n = -D_B\partial C/\partial z$, respectively.

In dimensionless form

$$\left\{\begin{array}{c} (\mathrm{Re}\cdot\bar{r}^2)^{1/2}C_{f\ r} = \dfrac{1}{1 + (\Gamma^2(F'(0)^2 + G'(0)^2))^{n/2}}, \\ (\mathrm{Re}\cdot\bar{r}^2)^{1/2}C_{f\ \theta} = \dfrac{1}{1 + (\Gamma^2(F'(0)^2 + G'(0)^2))^{n/2}}, \\ (\mathrm{Re}\cdot\bar{r}^2)^{-1/2}\mathrm{Nu} = -\theta'(0), \\ (\mathrm{Re}\cdot\bar{r}^2)^{-1/2}\mathrm{Sh} = -\varphi'(0). \end{array}\right\} \quad (36)$$

2 Comparison of the current method

A comparison through Table 1 exhibits exceptional matching with already available works, as presented in previous

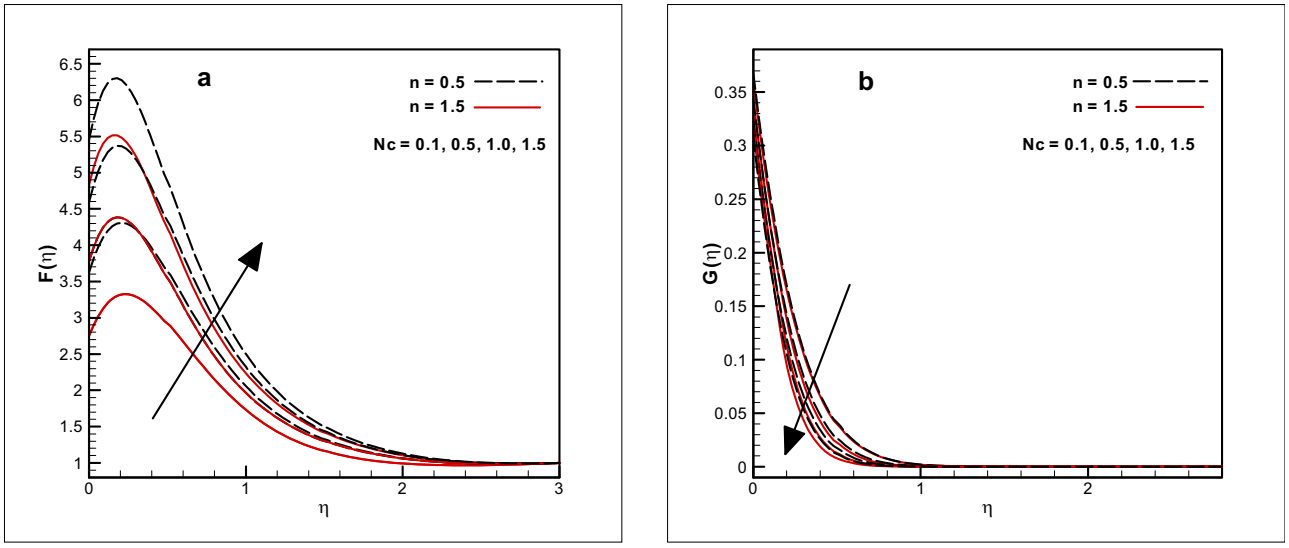

Figure 4: Impact of Nc on (a) $F(\eta)$ and (b) $G(\eta)$.

literature [7–9]. It is demonstrated that the following method is perfectly implemented with excellent accuracy. However, the comparison of this work is provided in limited cases, because the leading Eqs. (23)–(28) with BC's are very time-consuming for suitable expression while examining the flow conducts by considering all the leading impacts.

3 Results analysis

The interpretation of various physical characteristics is examined by taking different values of pertinent parameters. By keeping in view the three cases of GNF, *i.e.*, $0 < n < 1$ for pseudo plastic, $n = 1$ for Newtonian, and $n > 1$ for dilatant fluids. For the overall approximation findings, the fixed ranges for each parameter are specified as: $\Gamma = 0.01$; Pr = 0.3; Sc = 0.1; Ec = 0.1; $\lambda_1 = 0.5$; $\lambda_1 = 0.5$; $M = 2.0$; Ri = 50; Nc = 0.001.

Figure 2(a)–(d) illustrates the effect of the magnetic parameter and velocity slip on the velocity field, represented by (η) and $G(\eta)$, respectively. From the figures, it is noted that for ascending magnitude of M, the radial and tangential velocities of the fluid are diminished. Physically, magnetic field generates a type of forces called Lorentz forces, which is a type of resistive force that reduces the

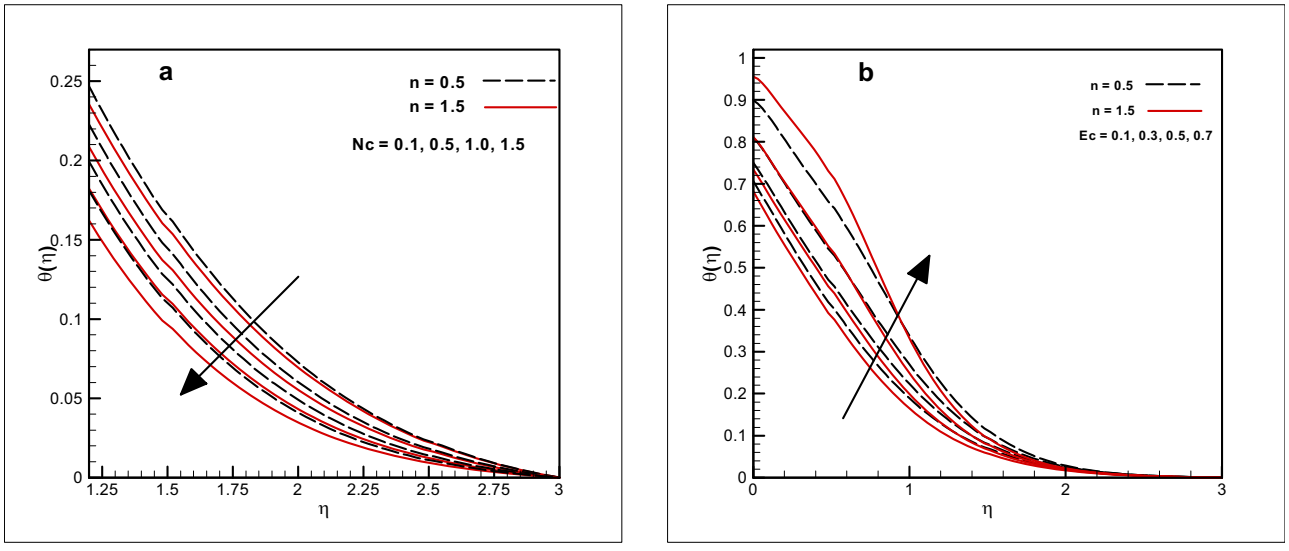

Figure 5: Impact of (a) Nc and (b) Ec on (η).

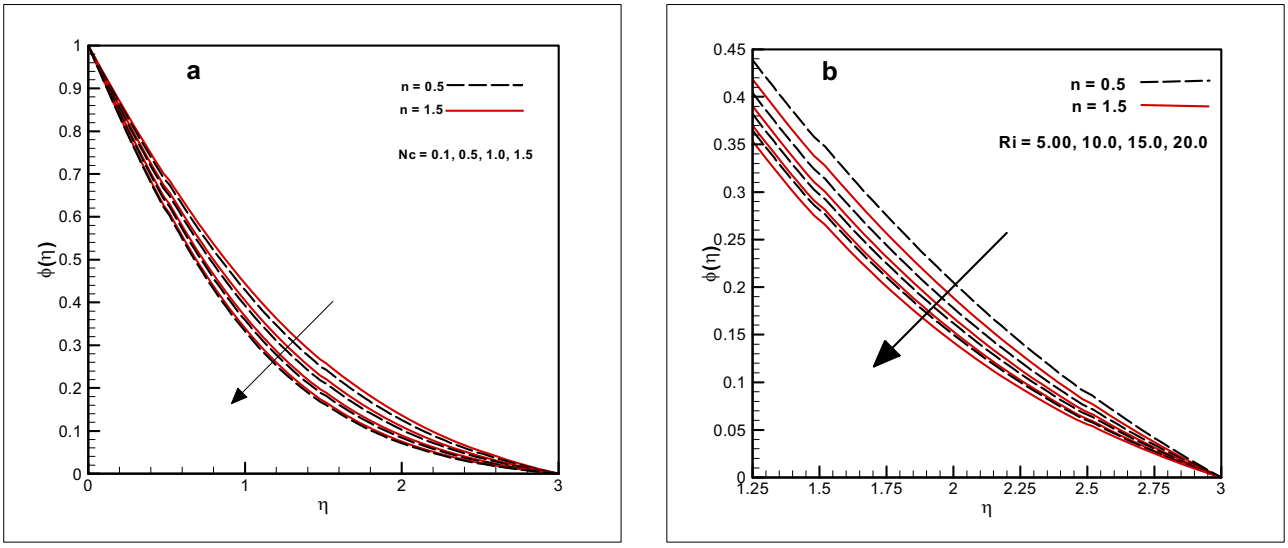

Figure 6: Impact of (a) Nc and (b) Ri on $\varphi(\eta)$.

fluid velocity. The uplifted values of λ_1, caused an escalation in the radial velocity and declined is noticed in the tangential velocity of the fluid. Actually, velocity slip reduced the drag and viscous forces that typically slow down the fluid near the boundary, allowing the fluid to move faster along the boundary. Figure 3(a)–(d) shows the impact of (Ri) on the velocity and temperature profile, respectively, *i.e.*, (η), $G(\eta)$, $H(\eta)$, and $\theta(\eta)$. The figures show that the higher (Ri) values improved the redial velocity but diminished the fluid's tangential and azimuthal velocities and temperature as well. In general, the influence of (Ri) in the vertically spinning disk is an exceptional one that boosts the velocity whenever increasing directly. The fluid velocity in the radial direction shows differences as corresponding to the tangential and the azimuthal velocities, *i.e.*, (η) and $H(\eta)$, respectively. The patterns of both fields (η) and $G(\eta)$ regarding the higher intensity of (Nc) parameter are manifested in Figure 4(a) and (b). These graphs yield the result that the larger values of (Nc) enhanced the radial velocity and declined the fluid's tangential velocity in the context of both shear thinning and shear thickening fluids. Physically, an increase in the buoyancy ratio parameter enhances radial velocity as the dominant solutal buoyancy forces drive stronger radial convection currents. Conversely, an increase in the buoyancy ratio parameter decreases tangential velocity because the energy is redirected toward

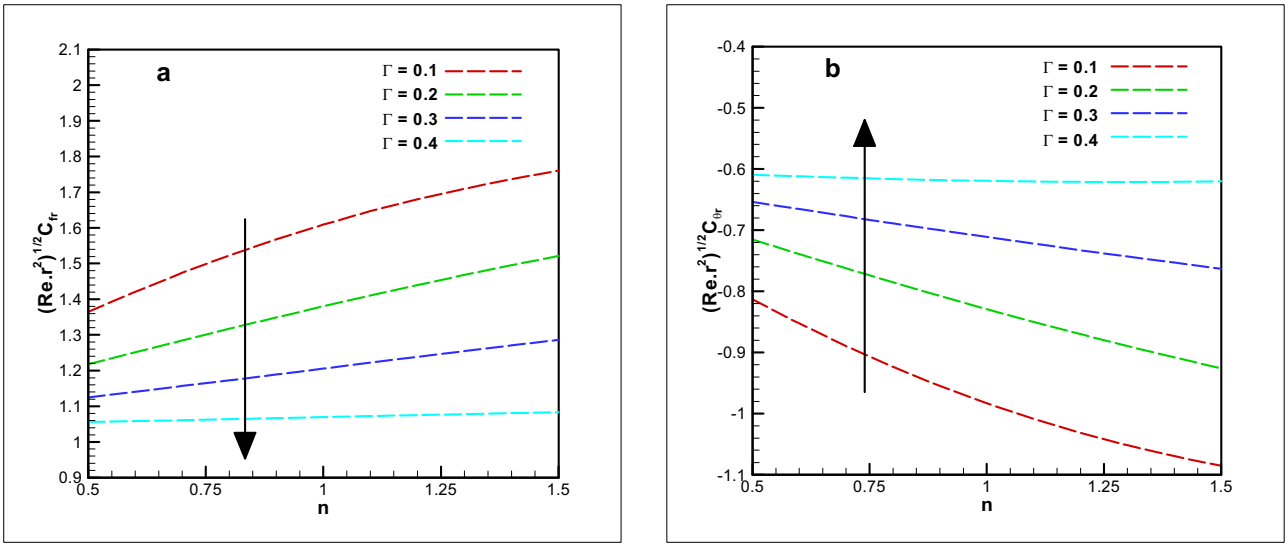

Figure 7: (a) and (b) Influence of Γ on $(\mathrm{Re}\cdot\bar{r}^2)^{1/2}C_{f\ r}$.

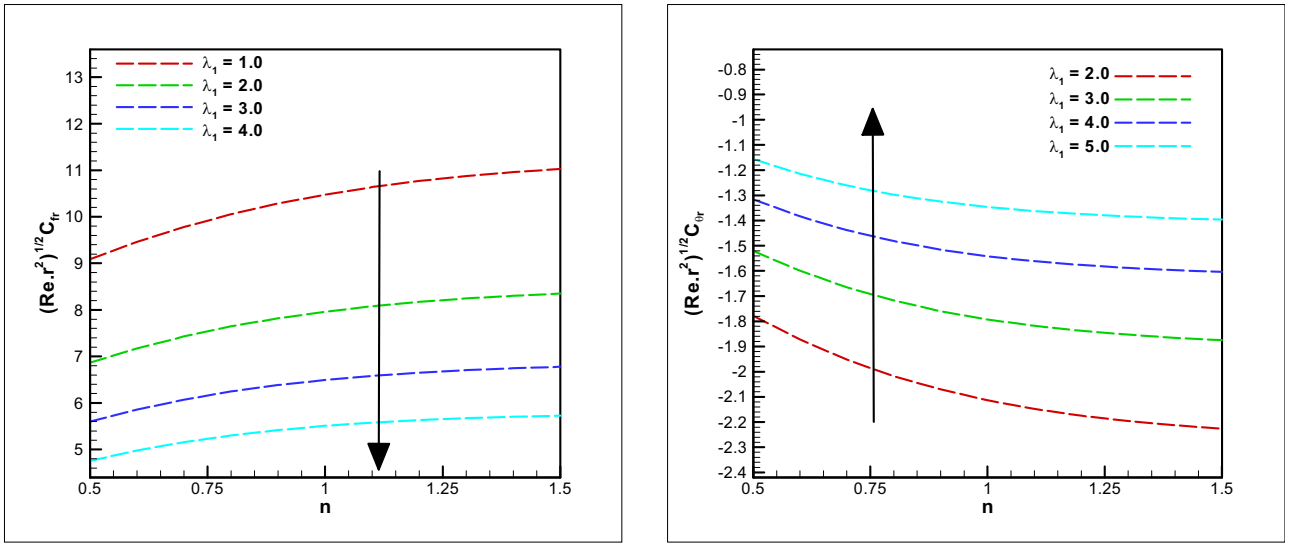

Figure 8: (a) and (b) Influence of λ_1 on $(\mathrm{Re}\cdot\bar{r}^2)^{1/2}C_{f\ \theta}$.

enhancing radial flow, and the system becomes more stabilized against the rotational instabilities. Figure 5(a) and (b) depicts the effects of the buoyancy ratio parameter and Eckert number on the pattern of the temperature. From the figures, larger values of (Nc) reduced the temperature of the fluid. Physically, when the buoyancy ratio increases, it indicates that the concentration effects become more dominant compared to the temperature effects. This can suppress the temperature-driven buoyant forces, leading to a weaker thermal convection, which can lower the overall temperature difference in the fluid as the temperature gradients diminished. But, on other hand, the ascending values of Ecker number increased the fluid temperature. Physically, it is defined as the ratio of kinetic energy and enthalpy. The uplifted values of Eckert number signifies that a greater proportion of the fluid's kinetic energy is being converted into thermal energy due to viscous dissipation, which in turn raises the temperature of the fluid. The impacts of buoyancy ratio parameter (Nc) and Richardson number on concentration is shown in Figure 6(a) and (b). From the figures, the ascending values of Nc declined the concentration of the fluid, because when we decrease the buoyancy ratio parameter, the thermal buoyancy dominates over solutal buoyancy. This stronger thermal convection enhances mixing, which tends to reduce concentration gradients. And it is the same for Richardson number, the ascending values of Ri diminished the concentration of the liquid. Physically, when the Richardson number increases, the buoyancy-driven convection dominates, leading to less horizontal mixing and more stratification. This reduces the effectiveness of mixing causing concentration to remain localized in specific regions and reduce the overall concentration in the fluid. Figure 7(a) and (b) demonstrates the influence of the relaxation time constant on the radial and tangential skin friction coefficients. The high values of (Γ) maximizing the radial skin friction and a reverse action were perceived for tangential friction drag. Physically, a higher relaxation time indicates that the material retains its deformed state for a longer period before relaxing. When such a fluid flows through a pipe or around an object, radial deformation (compression or expansion perpendicular to the flow) induces an elastic response. The longer relaxation time means that this elastic response is sustained longer, increasing resistance to radial deformation and thus increasing radial friction. An increased relaxation time constant results in a slower response to shear stresses, leading to reduced immediate resistance to tangential deformation. This manifests as lower effective viscosity, increased slip at the boundary, distributed shear forces over time, and ultimately decreased tangential skin friction. Figure 8(a) and (b)

Table 2: Impact of Ec on Nusselt number and Nc, Ri on Sherwood number

Ec	Nc	Ri	$(\mathrm{Re}\cdot\bar{r}^2)^{0.5}\mathrm{Nu}$	$(\mathrm{Re}\cdot\bar{r}^2)^{0.5}\mathrm{Sh}$
0.1	—	—	0.188772	—
0.2	—	—	0.521255	—
0.3	—	—	1.411790	—
—	0.1	—	—	0.671517
—	0.2	—	—	0.682423
—	0.3	—	—	0.692853
—	—	0.1	—	0.466369
—	—	0.2	—	0.467227
—	—	0.3	—	0.468076

shows the impact of velocity slip parameter λ_1 on redial and tangential skin fraction. Here the velocity slip increases the radial skin friction and *vice-versa* for tangential skin friction. Physically, the reduction in the radial skin friction with the variation in velocity slips is due to the decline in the velocity gradient and which decreases the shear stress. And hence alters the boundary layer and minimize the momentum transfer between the fluid and the solid boundary. These factors together result in less resistance to the flow, which manifests as reduced skin friction. Velocity slip decreases the tangential velocity profile because it reduces the velocity gradient, weakens the momentum transfer between the boundary and the fluid, and alters the boundary layer dynamics. Table 2 shows the impact of Eckert number on Nusselt and the buoyancy ratio parameter and Richardson number on Sherwood number. The higher value of Ec increases the Nusselt number. In general, the Eckert number represents the ratio of kinetic energy to the enthalpy differences in a fluid flow. When the Eckert number increases, the kinetic energy of the fluid becomes more significant relative to the temperature difference, and this can lead to an enhancement in the Nusselt number. The larger values of Nc and Ri enhanced the Sherwood number. Both the buoyancy ratio and Richardson number increase natural convection processes. This enhancement of convective forces leads to better mass transfer, reflected by an increase in the Sherwood number.

4 Conclusion

The dissipative flow pattern of rheological material has been examined to address the energy loss. A typical rotating stagnation point flow of Cross materials has been analyzed in the presence of thermal radiation, mixed convection, and magnetic force. The significant viscous dominant flow analysis explored the concept of boundary layer region flow. The gravitationally effected flow pattern has been phenomenal during the approximation of different physical features including material rotating speed, thermal flow, mass flow, surface resistance, mass, and heat rate flows. Every new finding was effective in the practical sense while exploring the physical features of the newly modeled problem. A difference in the surface velocity, surface temperature, material velocity, and temperature was assumed in the spinning motion of the generalized Cross materials. The material speed, concentration, temperature, surface force, pressure, and flow rates of mass and heat are graphically interpreted with variation in various physical factors. A well-matched comparison was reported to show the accuracy of the implemented method. The entire study has been very significant in terms of its key findings, which are listed below.

- The fluctuation in Richardson number enhanced the radial component of liquid velocity, while the other components showed opposite tendencies.
- The flow slip factor enhanced the radial flow speed of the material and an opposite demeanor was detected in the case of tangential flow speed.
- The purpose of the augmentation of the Lorentz forces factor is to deteriorate the movement of the considered fluid.
- The flow speed has been enhanced for higher relaxation factor Γ and by considering the shear thinning and thickening cases.
- The radial and tangential resistive forces declined and enhanced, respectively, by varying the relaxation time constant Γ.
- The dissipative Eckert number enhanced the material temperature significantly.
- The pressure of the material has been noticed higher for the growing values of the Richardson number.

Acknowledgments: Princess Nourah bint Abdulrahman University Researchers Supporting Project number (PNURSP2025R908), Princess Nourah bint Abdulrahman University, Riyadh, Saudi Arabia.

Funding information: Princess Nourah bint Abdulrahman University Researchers Supporting Project number (PNURSP2025R908), Princess Nourah bint Abdulrahman University, Riyadh, Saudi Arabia.

Author contributions: Conceptualization: L.A. and S.I.; methodology: L.A. and S.I.; validation: M.Y. and S.I.; formal analysis: S.I. and M.Y.; investigation: S.I. and U.K.; resources: J.A.B. and U.K.; data curation: L.A. and S.I.; writing – original draft preparation: S.I. and L.A.; writing – review and editing: L.A. and M.Y.; visualization: S.I. and U.K.; and supervision: L.A. and J.A.B. All authors have accepted responsibility for the entire content of this manuscript and approved its submission.

Conflict of interest: The authors state no conflict of interest.

Data availability statement: The datasets generated and/or analyzed during the current study are available from the corresponding author on reasonable request.

References

[1] Bilal S, Shah IA, Akgül A, Tekin MT, Botmart T, Yousef ES, et al. A comprehensive mathematical structuring of magnetically effected Sutterby fluid flow immersed in dually stratified medium under boundary layer approximations over a linearly stretched surface. Alex Eng J. 2022;61(12):11889–98.

[2] Qureshi ZA, Bilal S, Khan U, Akgül A, Sultana M, Botmart T, et al. Mathematical analysis about influence of Lorentz force and interfacial nano layers on nanofluids flow through orthogonal porous surfaces with injection of SWCNTs. Alex Eng J. 2022;61(12):12925–41.

[3] Rehman KU, Malik MY, Khan WA, Khan I, Alharbi SO. Numerical solution of non-Newtonian fluid flow due to rotatory rigid disk. Symmetry. 2019;11(5):699.

[4] Kármán TV. Über laminare und turbulente Reibung. ZAMM-J Appl Math Mech/Z Angew Math Mech. 1921;1(4):233–52.

[5] Turkyilmazoglu M, Senel P. Heat and mass transfer of the flow due to a rotating rough and porous disk. Int J Therm Sci. 2013;63:146–58.

[6] Ahmed SE, Arafa AA, Hussein SA. Bioconvective flow of a variable properties hybrid nanofluid over a spinning disk with Arrhenius activation energy, Soret and Dufour impacts. Numer Heat Transf, Part A: Appl. 2024;85(6):900–22.

[7] Arafa AA, Hussein SA, Ahmed SE. Hydrothermal bioconvective Bödewadt ternary composition nanofluids flow over a stretching rotating disk through a heat generating porous medium. J Magn Magn Mater. 2023;586:171174.

[8] Turkyilmazoglu M. Heat and mass transfer on the MHD fluid flow due to a porous rotating disk with Hall current and variable properties. J Heat Transf. 2011;133(2):021701.

[9] Cross MM. Rheology of non-Newtonian fluids: a new flow equation for pseudoplastic systems. J Colloid Sci. 1965;20(5):417–37.

[10] Andersson HI, De Korte E, Meland R. Flow of a power-law fluid over a rotating disk revisited. Fluid Dyn Res. 2001;28(2):75.

[11] Khan M, Salahuddin T, Chu YM. Analysis of the Carreau fluid model presenting physical properties along different molecular axes near an anisotropic rough surface. Int Commun Heat Mass Transf. 2021;123:105233.

[12] Ming C, Liu K, Han K, Si X. Heat transfer analysis of Carreau fluid over a rotating disk with generalized thermal conductivity. Comput Math Appl. 2023;144:141–9.

[13] Raji A, Hasnaoui M, Bahlaoui A. Numerical study of natural convection dominated heat transfer in a ventilated cavity: Case of forced flow playing simultaneous assisting and opposing roles. Int J Heat Fluid Flow. 2008;29(4):1174–81.

[14] Nasseri L, Ameziani DE, Rahli O, Bennacer R. Numerical study of mixed convection in a ventilated square enclosure with the lattice Boltzmann method. Numer Heat Transf, Part A: Appl. 2019;75(10):674–89.

[15] Singh S, Sharif MAR. Mixed convective cooling of a rectangular cavity with inlet and exit openings on differentially heated side walls. Numer Heat Transf: Part A: Appl. 2003;44(3):233–53.

[16] Abu-Nada E, Chamkha AJ. Mixed convection flow of a nanofluid in a lid-driven cavity with a wavy wall. Int Commun Heat Mass Transf. 2014;57:36–47.

[17] Kalteh M, Javaherdeh K, Azarbarzin T. Numerical solution of nanofluid mixed convection heat transfer in a lid-driven square cavity with a triangular heat source. Powder Technol. 2014;253:780–8.

[18] Garoosi F, Garoosi S, Hooman K. Numerical simulation of natural convection and mixed convection of the nanofluid in a square cavity using Buongiorno model. Powder Technol. 2014;268:279–92.

[19] Turkyilmazoglu M, Pop I. Rheology of Bingham viscoplastic flow triggered by a rotating and radially stretching disk. Int J Numer Methods Heat Fluid Flow. 2025;35(2):847–63.

[20] Yasmin H, Mahnashi A, Hamali W, Lone S, Raizah Z, Saeed A. A numerical analysis of the blood-based Casson hybrid nanofluid flow past a convectively heated surface embedded in a porous medium. Open Phys. 2024;22(1):20230193. doi: 10.1515/phys-2023-0193.

[21] Navier CLMH. Mémoire sur les lois du mouvement des fluides. Mém Acad Roy Sci Inst France. 1823;6(1823):389–440.

[22] Maxwell JC. The scientific papers of James Clerk Maxwell. Vol. 2. Cambridge: Cambridge University Press; 1890.

[23] Hayat T, Khan MI, Waqas M, Yasmeen T, Alsaedi A. Viscous dissipation effect in flow of magnetonanofluid with variable properties. J Mol Liq. 2016;222:47–54.

[24] Mathur P, Mishra SR, Pattnaik PK, Dash RK. Characteristics of Darcy–Forchheimer drag coefficients and velocity slip on the flow of micropolar nanofluid. Heat Transf. 2021;50(7):6529–47.

[25] Motsa SS, Khan Y, Shateyi S. A new numerical solution of Maxwell fluid over a shrinking sheet in the region of a stagnation point. Math Probl Eng. 2012;2012(1):290615.

[26] Turkyilmazoglu M. Slip flow between corotating disks with heat transfer. Int J Numer Methods Heat Fluid Flow. 2025;35(1):257–76.

[27] Yasmin H, Bossly R, Alduais F, Al-Bossly A, Saeed A. Water-based hybrid nanofluid flow containing CNT nanoparticles over an extending surface with velocity slips, thermal convective, and zero-mass flux conditions. Open Phys. 2025;23(1):20250122. doi: 10.1515/phys-2025-0122.

[28] Asghar A, Dero S, Lund L, Shah Z, Alshehri M, Vrinceanu N. Slip effects on magnetized radiatively hybridized ferrofluid flow with acute magnetic force over shrinking/stretching surface. Open Phys. 2024;22(1):20240052. doi: 10.1515/phys-2024-0052.

[29] Gupta AS. Laminar free convection flow of an electrically conducting fluid from a vertical plate with uniform surface heat flux and variable wall temperature in the presence of a magnetic field. Z Angew Math Phys ZAMP. 1962;13:324–33.

[30] Gebhart B, Mollendorf J. Viscous dissipation in external natural convection flows. J Fluid Mech. 1969;38(1):97–107.

[31] Boutoutaou H, Fontaine JF. Methodology of a computer aided design of shrink fit taking into account roughness and form defects of manufacturing process. J Mech Sci Technol. 2015;29(5):1–7.

[32] Soundalgekar VM, Murty TR. Heat transfer in MHD flow with pressure gradient, suction and injection. J Eng Math. 1980;14:155–9.

[33] Ahmed SE, Raizah ZA, Hafed ZS, Morsy Z. Hall and ohmic heating effects on radiative flow of viscoelastic nanofluids over a convective rotating rigid/stretched disk. Case Stud Therm Eng. 2024;55:104154.

[34] Ontela S, Musala V, Ahmed SE, Thumma T. Optimization and sensitivity analysis on axisymmetric motile microorganism flow of viscoelastic nanofluid over a spinning circular disk with a central composite model. Numer Heat Transf, Part A: Appl. 2024;85(23):3956–81.

[35] Ali F, Zahid M, Souayeh B, Asmat F, Nwaigwe C. Analytical and numerical investigation for viscoelastic fluid with heat transfer analysis during rollover-web coating phenomena. Open Phys. 2024;22(1):20240024. doi: 10.1515/phys-2024-0024.

[36] Wang Z, Wang S, Wang X, Luo X. Permanent magnet-based superficial flow velometer with ultralow output drift. IEEE Trans Instrum Meas. 2023;72:1–12. doi: 10.1109/TIM.2023.3304692.
[37] Guo H, Li Y, Zhao B, Guo Y, Xie Z, Morina A, et al. Transient lubrication of floating bush coupled with dynamics and kinematics of cam-roller in fuel supply mechanism of diesel engine. Phys Fluids. 2024;36(12):123103. doi: 10.1063/5.0232226.
[38] Wang L, Xiao K, Xiang G, Cai J, Yang T, Wang J. Study on mixed thermal-visco-hyperelastic hydrodynamic lubrication performance of water-lubricated rubber bearings in deep-sea environment. Tribol Int. 2025;209:110713. doi: 10.1016/j.triboint.2025.110713.
[39] Chen X, Cui J, Liu Y, Zhang X, Sun J, Ai R, et al. Joint scene flow estimation and moving object segmentation on rotational LiDAR data. IEEE Trans Intell Transp Syst. 2024;25(11):17733–43. doi: 10.1109/TITS.2024.3432755.
[40] Yang Y, Li H. Neural ordinary differential equations for robust parameter estimation in dynamic systems with physical priors. Appl Soft Comput. 2024;169:112649. doi: 10.1016/j.asoc.2024.112649.